IEEE Access
Multidisciplinary ⋮ Rapid Review ⋮ Open Access Journal

Received 1 October 2023, accepted 19 October 2023, date of publication 25 October 2023, date of current version 10 November 2023.

Digital Object Identifier 10.1109/ACCESS.2023.3327638

METHODS

Capability of AgSiN/SU-8 Layer on Silver-Based SPR for Adulterated Honey Detection

M. B. JAAFAR[1], M. B. OTHMAN[1], (Member, IEEE), M. M. I. MEGAT HASNAN[2], AND H. HAROON[3], (Member, IEEE)

[1]Faculty of Electrical and Electronic Engineering, Universiti Tun Hussein Onn Malaysia (UTHM), Batu Pahat, Johor 86400, Malaysia
[2]Faculty of Engineering, University Malaysia Sabah (UMS), Kota Kinabalu, Sabah 88400, Malaysia
[3]Faculty of Electronic and Computer Engineering, Universiti Teknikal Malaysia Melaka (UTeM), Durian Tunggal, Melaka 76100, Malaysia

Corresponding author: M. B. Othman (maisara@uthm.edu.ny)

This research was supported by Universiti Tun Hussein Onn Malaysia (UTHM) through Tier 1 (vot Q485).

ABSTRACT This study introduces the capability of the AgSiN/SU-8 layer on the silver-based SPR structure for water content detection in stingless bee honey. The 30% water content in pure honey was adulterated by water bath procedure until they reached 18% adulterated honey. The experiment was carried out for two different SPR structures, with and without AgSiN/SU-8 layer to examine its potential in protecting the silver metal from eroding and minimize the formation of the silver oxide. The resonance angles of adulterated honey solutions for these two SPR structures denote a similar behavior by shifting to a higher angle from the pure honey solution. It indicates that the AgSiN/SU-8 layer can select and detect the variation percentage of honey water content. After 24 hours, the Cr/Ag/AgSiN/SU-8 structure produces the equivalent resonance angle value with only 5.26% changes in minimum reflectivity. It shows that the AgSiN/SU-8 layer can protect the silver surface from erosion and preserve the SPR characteristic. Besides, the presence of the AgSiN/SU-8 layer on the silver surface is capable of decreasing the oxygen atomic percentage by 21.48%, hence minimizing the growth of silver oxide. This work is a preliminary study of the AgSiN/SU-8 layer to detect water content in stingless bee honey, at the same time can protect the silver surface from erosion and minimize the formation of the silver oxide.

INDEX TERMS Silver-silicon nitride, SU-8 photoresist film, surface plasmon resonance, honey adulteration detection, protective layer.

I. INTRODUCTION

Stingless bee honey is a natural food sweetener produced by the stingless bees that considered to have higher nutritional and medicinal value compared to the other honeybees [1]. It is a viscous and complex solution mainly composed of sugar and water with a small amount of other compounds, such as amino acids, enzymes, organic acids, minerals, vitamins, pollen, and proteins [1], [2], [3], [4], [5]. Stingless bee honey has higher water content compared to the honey of sting bees [4], [6], [7]. The water content in honey varies depending on how it is harvested, stored, and environment, which can affect the physical characteristics of honey, such as crystallization and viscosity.

The associate editor coordinating the review of this manuscript and approving it for publication was Leo Spiekman.

According to the Codex regulation [8], commercial honey is a pure product with no other ingredients and particular constituents being added or removed from it. However, the restricted production level of stingless bee honey and the lack of international standards have put pure honey into an adulteration issue [7]. Adulteration of honey causes a reduction in the natural therapeutic value of honey. To overcome this challenge, various analytical techniques have been introduced to appraise the authenticity of honey including spectroscopic [9], [10], [11] chromatographic [12], [13], [14], isotope analysis [15], [16], and physico-chemical analysis. These conventional approaches are useful and accurate in identifying the honey authenticity, but involving high knowledge to handle the devices, time-consuming, and expensive instruments. Hence, several researchers have designed optical sensing devices for adulterated honey detection since it is simple, rapid, and chemical-free approach [17], [18], [19], [20].

The optical phenomenon of surface plasmon resonance (SPR) has recently drawn huge attention among the research community due to its high-potential in the area of optical sensing, biomedicine, and electronics. Since SPR is a non-radiative and label-free detection method, it is well-suited for numerous applications in chemical and biological sensing, including the detection of adulterated honey [21]. SPR refers to the optical excitation of surface plasmons (SPs) at the interface between a metal and a dielectric. The SPR technique is based on the electromagnetic response relying on the variation in refractive index that occurred on the sensing surface due to the adsorption of the target analyte.

Noble metals such as gold, silver, and copper are the most commonly used for SPR applications. In this regard, even though gold possesses high chemical stability, silver is preferred since it exhibits higher conductivity and a sharper resonance spectrum than gold and copper metal. However, silver metal may cause the sensing surface to be easily oxidized [22], [23] due to the presence of oxygen element. The growth of silver oxide layer can produce a broader SPR curve width [24]. The oxidation and stability issues of plasmonic materials can be solved by protecting the metal surface with a thin and inert layer that is impermeable to water, oxygen, and other corroding agent [23]. For instance, the bimetallic layer [25], two-dimensional (2D) structures of graphene [26], [27] and molybdenum disulfide [28], [29], and wurtzite nitride semiconductor [30], [31], [32] have been proposed as protective elements against metal corrosion. In addition to this, the thickness of noble metal can also affect the strength of SPR signal. The power of energy transferred from the excitation beam to the SPs wave becomes weaker with the thicker metal thickness. An ideal metal thickness to excite surface plasmons is within the range of 40 nm to 60 nm.

In this study, the capability of silver-silicon nitride (AgSiN) and SU-8 photoresist film for water content detection in stingless bee honey are introduced to protect the silver metal from eroding [33] and simultaneously minimize the formation of the silver oxide. The experiment was carried out for two different SPR structures, with and without AgSiN/SU-8 layer, as shown in Figure 1. The SPR structures were analyzed based on the Energy Dispersive Spectroscopy (EDS), surface morphology, and Tauc plot analysis. The narrowness and depth of the SPR curves were observed and evaluated in terms of sensitivity and full width at half maximum (FWHM). This is the first study of AgSiN and SU-8 film for honey water content detection using silver-based SPR technique.

II. SPR THEORETICAL CONCEPT

Plasma is a fourth fundamental state of matter that contains a portion of charged particles; ions and electrons. Collective oscillations of plasma propagating in a bulk metal are called plasmons. Plasmons are created by the interaction of charged particles at the plasma frequency, where the fixed positive ions in a metal exert an attractive force on the free electrons to pull them back to their original position. The plasma frequency, ω_p is defined as the natural oscillation frequency of the electrons with respect to the ions.

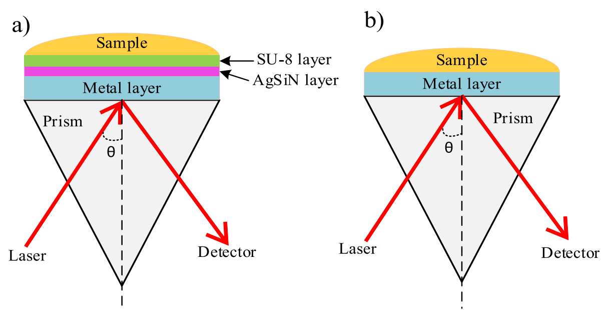

FIGURE 1. SPR structures (a) with and (b) without AgSiN/SU-8 layer.

$$\omega_p = \sqrt{\frac{Ne^2}{\varepsilon_0 m_e}} \tag{1}$$

The subscript N is the electron density, $e$is the electron charge, ε_0 is the permittivity of vacuum, and m_e is the electron mass. In contrast to bulk plasmons that oscillate throughout the bulk metal, surface plasmons (SPs) are subjected to longitudinal charge density oscillations at the interface between a metal and dielectric with opposite signs in a real part of dielectric permittivity, as shown in Figure 2. The propagation of surface plasmon polaritons (SPPs) take place when the charge motion in SPs interacts strongly with electromagnetic radiation. SPPs are electromagnetic waves composed of surface charges propagating along the metal-dielectric interface. The wave travels along the x-direction and exponentially vanishes the amplitude in the direction perpendicular to the interface. In the z-direction, the decay length or skin depth into the dielectric, δ_d and metal, δ_m are reduced by a factor of $1/e$.

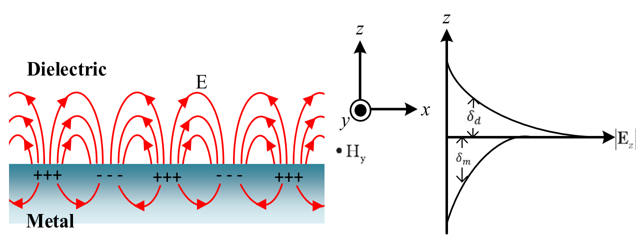

FIGURE 2. Schematic diagram of the electromagnetic field for SPs propagating along metal and dielectric interface.

The conservation laws of both momentum and energy must be fulfilled to excite the SPPs. The relation between the momentum in terms of the wavevector in the propagation direction k_x and the energy in the angular frequency ω is plotted in Figure 3. The excitation of SPPs can be established by coupling the wavevector component of the incident light (k_x)

and the propagation constant of surface plasmons (k_{sp}).

$$k_x = \frac{\omega}{c} n_p \sin\theta_i \quad (2)$$

$$k_{sp} = \frac{\omega}{c}\sqrt{\left(\frac{\varepsilon_m \varepsilon_d}{\varepsilon_m + \varepsilon_d}\right)} \quad (3)$$

where ω, n_p, c, and θ_i correspond to the angular frequency, refractive index of the glass prism, velocity of light, and the incident angle. While the ε_m and ε_d denote to the permittivity of metal and dielectric. It should be noted that the k_{sp} is always greater than that of the wavevector of freely propagating photon (ω/c). Conceptually, the surface plasmons can be excited through evanescent waves created inside a medium of refractive index ($n >1$) with an incident angle larger than the critical angle. In this situation, the slope of the tilted light line in medium, $\omega = ck_x/n$ is lowered and intersect with the surface plasmon curve.

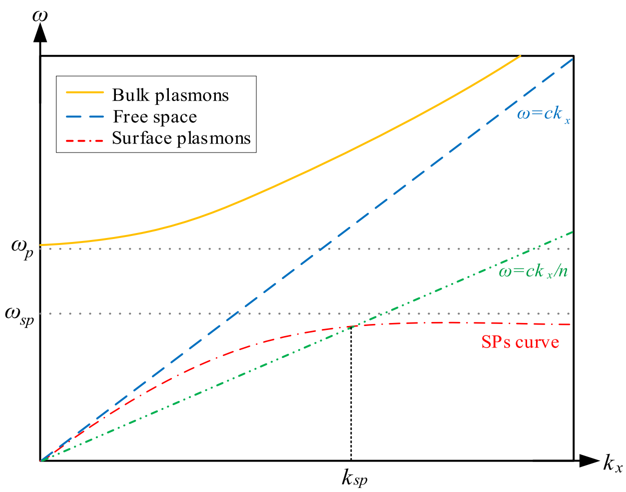

FIGURE 3. Dispersion relation of surface plasmons.

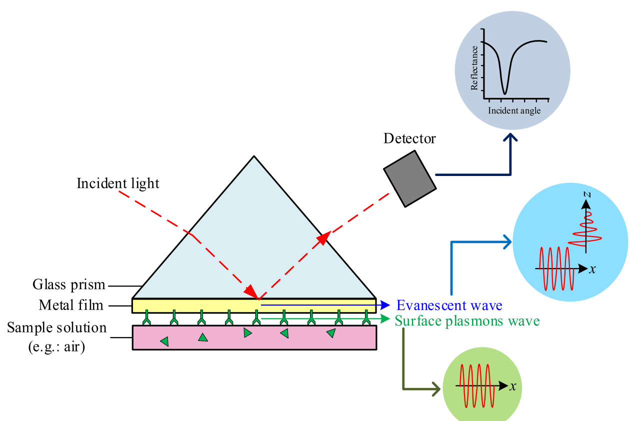

FIGURE 4. Schematic illustration of the principle of the SPR system.

Surface plasmons resonance occurs when the electrons in the metal surface are excited by the photon of parallel polarized (p-polarized) light under total internal reflection situations. The electromagnetic field component of the incident radiation penetrates up to a certain distance from a medium with a high refractive index into the lower refractive index, such as a glass-air medium, creating an exponentially decaying evanescent wave, as illustrated in Figure 4. The polarization of the evanescent field wave can interact with the free electrons of the thin metal layer coated in between the medium interface, hence resulting in the excitation of surface plasmon waves propagating on the metal surface. The resonance energy transfer between the evanescent wave and surface plasmons produces a minimum intensity of the reflected radiation at a particular incident angle due to the energy losses during the transmission coupling of photons to the plasmons.

III. METHODOLOGY

A. MATERIALS

The three elements targets that are chromium (Cr), silver (Ag) and silicon (Si) with the purity of 99.95% were purchased from Nanorian Technologies Sdn. Bhd. The SU-8 3000 negative photoresist laminate film with the refractive index of n = 1.567 was acquired from Kayaku Advance Material Japan. A 20 mm × 20 mm × 20 mm right-angle BK-7 glass prism with refractive index, n = 1.51 obtained from Bohr Optic Co. Ltd. was used as a substrate.

B. SAMPLE PREPARATION

The authentic stingless bee honey was purchased from the established bee farm in the South region of Peninsular Malaysia, known as Asiana Bees Sdn. Bhd (ABSH), Johor. The 120 grams of pure honey were divided into four jar bottles, where the three bottles were ready for adulterated honey. The adulterated honey samples were prepared by deliberately reducing the water content in honey through the water bath procedure with a temperature between 80°C to 85°C. The evaporation process that occurred during the water bath procedure has decreased the water content in honey samples from 30% pure honey (0% adulterant volume) to 18% adulterated honey (12% adulterant volume).

C. FABRICATION OF SPR STRUCTURE

The fabrication procedure of the proposed SPR structure is displayed in Figure 5, which comprises the simple cleaning process, the thin film deposition and, and the SU-8 lamination process. First, the prism substrate was sonicated with acetone, followed by isopropyl ethanol (IPA) for 10 minutes at 30°C each, to remove the contaminants from the substrate using the ultrasonic bath. Then, the substrate was rinsed with deionized (DI) water and dried using drying oven for 20 minutes at 70°C to evaporate the remaining solvent.

The next process is a deposition of the thin film using radio frequency (RF) magnetron sputtering technique, as prescribed in Table 1. The Ag and AgSiN films were sputtered on a chromium adhesion layer at the hypotenuse surface of the prism with the base pressure at 8×10^{-6} Torr. Argon gas

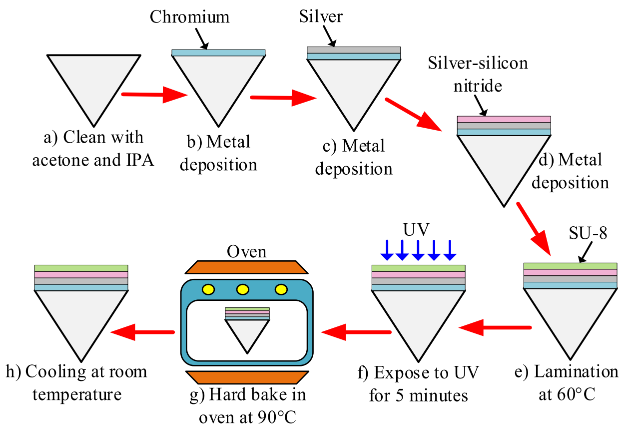

FIGURE 5. Fabrication procedure of the SPR structure.

pressure was set to 100 sccm with 100 W power source for Cr and Ag films. The AgSiN was deposited using Argon/Nitrogen gases mixture at 50 W and 200 W power of Argon and Nitrogen, individually. The working pressure for Ag and AgSiN were adjusted to 0.003 Torr with the deposition rate of 9.3487 s/nm and 2.0114 s/nm, respectively. While the working pressure for Cr was set to 0.005 Torr at the deposition rate of 15 s/nm. The profilometer confirmed that the thickness of the Cr, Ag, and AgSiN layers was approximately 1 nm, 32 nm, and 29 nm, respectively.

The final stage is the lamination process of the SU-8 photoresist film with the 3.9 μm fixed thickness on the deposited prism surface using a hot plate at the temperature of 60°C. The SU-8 surface was manually rolled out using a roller for better adhesion. Then, the laminated prism was exposed to the ultraviolet (UV) source of 1 mW for 5 minutes before the hard bake in the oven at 90°C for 10 minutes. Lastly, the laminated prism was cooled down at the ambient temperature and ready for the SPR testing.

TABLE 1. RF magnetron sputtering setting selection.

Material	Cr	Ag	AgSiN
Argon pressure (sccm)	100	100	100
Working pressure (Torr)	0.005	0.003	0.003
Base pressure (Torr)	8 x 10^{-6}	8 x 10^{-6}	8 x 10^{-6}
Power source (W)	100	100	Argon: 50 Nitrogen: 200
Deposition rate (s/nm)	15	9.3487	2.0114

D. EXPERIMENTAL PROCEDURE

An optical prism-coupled SPR structure is employed based on the Kretschmann prism configuration to couple the incident light at the attenuated total reflection for the SPR excitation, as illustrated in Figure 6. The incident light of a parallel polarized 650 nm laser diode with 0.005 Watt output power is propagated directly to a prism substrate on the rotation stage for the plasmons resonance activation. The angle of the incident light beam is controlled by the motorized rotating stage in a counter-clockwise direction with one degree (1°) angular resolution. The incident angle value, θ_i can be achieved from the following relation [34]:

$$\theta_i = arcsin \frac{\sin(\theta_{ex} - A_p)}{n_p} + A_p \tag{4}$$

where θ_{ex} is the external angle onto the prism surface, A_p is the angle of the prism specified in Figure 7 which equivalent to 45°, and the term n_p refers to a refractive index of the glass prism. The optical signal detection involves a photodetector to collect the reflected beam from the coated prism surface on a different degree of angle. Customized software consists of an analog-to-digital converter (ADC) and a gain amplifier interfaced to a computer to record and store the reflected light intensity as a function of incidence angle at a coated prism in real-time. The normalized reflectance is calculated where the reflectance is a ratio between the incident and reflected light intensity.

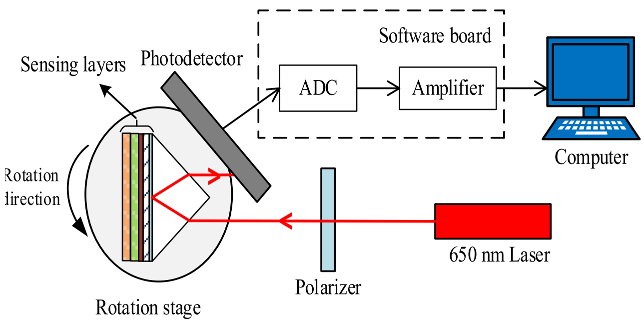

FIGURE 6. Schematic diagram of SPR experimental set up.

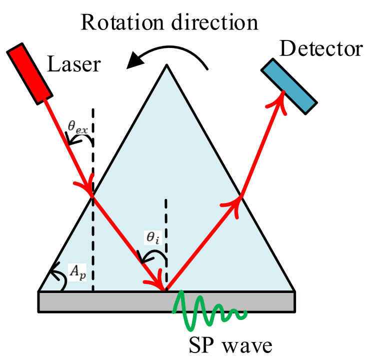

FIGURE 7. Internal and external angles of prism.

IV. RESULT AND DISCUSSION

A. SPR SENSING CURVE

The proposed SPR structures are illustrated in Figure 8, where the Cr/Ag layer is a reference model to a new Cr/Ag/AgSiN/SU-8 sensing structure. The SPR structure was initially verified on air (n=1.0) and DI water (n=1.33), followed by the honey solutions of 30%, 26%, 22%, and 18% water content. The SPR response against concentration divergence of adulterated honey using Cr/Ag and Cr/Ag/AgSiN/SU-8 sensing layer is depicted in Figure 9.

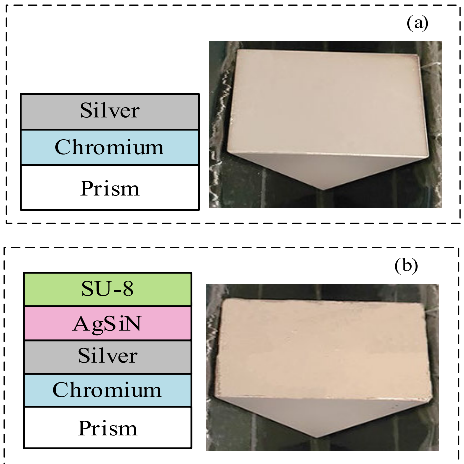

FIGURE 8. SPR sensing structure of (a) Cr/Ag and (b) Cr/Ag/AgSiN/SU-8 on the prism substrate.

The SPR curves for air, water, and honey samples show their own narrow dips at various resonance angles. The resonance dips occur due to the reaction of surface plasmons excitation that involves the transfer of energy from the incident photons [21]. The resonance angle for pure honey was observed at 66.85° and 65.26° in Cr/Ag and Cr/Ag/AgSiN/SU-8 structures, respectively. The distinct thickness of the SPR structure exhibits a varying resonance angle. In Cr/Ag structure, the resonance angles shift is 0.584°, 1.739°, and 2.875° for 26%, 22%, and 18% adulterated honey solutions, respectively. While the Cr/Ag/AgSiN/SU-8 structure shows the resonance angles shifting at 0.589°, 1.173°, and 1.753° for 26%, 22%, and 18% honey water content, respectively. The shift in resonance angle of adulterated honey reveals the capability of the SPR structures to select and detect the variation percentage of honey water content.

Theoretically, the SPR signal is sensitive to the refractive index of surrounding medium. A linear relationship is plotted in Figure 10 to determine the refractive index of the adulterated honey solutions. It has been confirmed that the refractive index of honey is in the range of 1.461 to 1.492, where the pure honey shows the lowest refractive index value. The decrement of honey water content led to the refractive index increment, hence shifting the SPR curve towards a higher angle. The result reports that the shift of resonance angles for different sensing samples is principally due to the variations in the refractive index, in which the bio-molecular interaction between the sensing surface and sample solution has exist [35].

However, after 24 hours, the SPR curves of the Cr/Ag structure shifted the resonance angle from the initial testing by 1.15°, 1.14°, and 0.56° for honey water contents

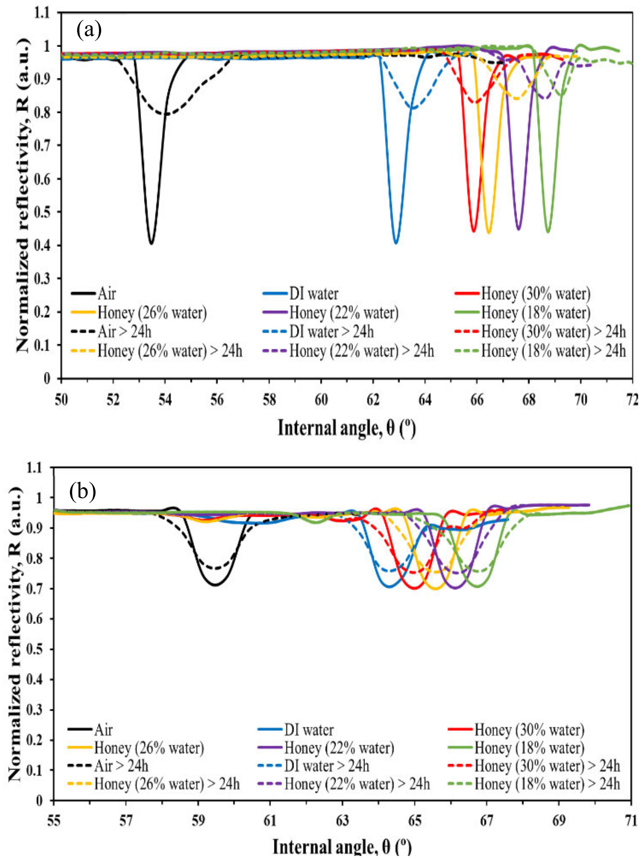

FIGURE 9. SPR curves for (a) Cr/Ag and (b) Cr/Ag/AgSiN/SU-8 sensing layers.

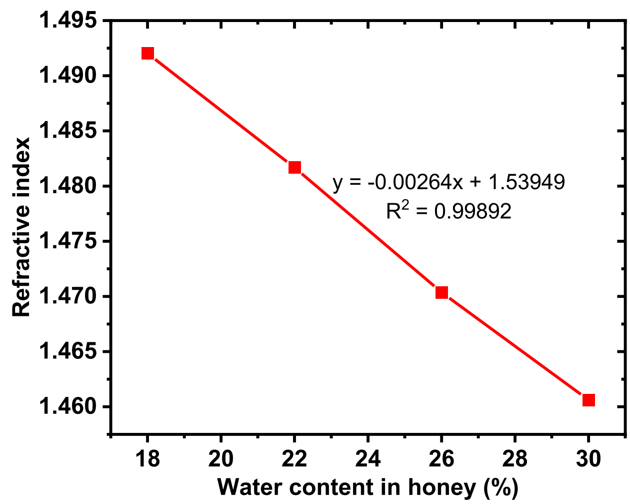

FIGURE 10. Refractive index against percentage of water content in honey.

of 26%, 22%, and 18%, respectively. The erosion reaction during cleaning process altered the SPR characteristic and thus amended the SPR curve drastically. In the meantime, the Cr/Ag/AgSiN/SU-8 structure displays similar resonance angles to the first application and no degradation occurred on the SPR sensing surface. The finding expresses that the AgSiN/SU-8 layer can protect the silver metal from eroding and shows a stable system that sustains the SPR characteristic by producing identical resonance angle values.

In the context of reflectivity, the 30%, 26%, 22%, and 18% water content of honey samples recorded the minimum reflection of 0.443, 0.438, 0.449, and 0.442 in Cr/Ag structure, respectively. On the other hand, the Cr/Ag/AgSiN/SU-8 structure has the minimum reflection of 0.724, 0.724, 0.720, and 0.731 for 30%, 26%, 22%, and 18% water content of honey, individually. The thickness of the silicon nitride that enables a range of colors to be produced [36] can influence the anti-reflection characteristic. The larger the thickness of the silicon nitride layer, the higher the value of reflection.

Nevertheless, the SPR curves of Cr/Ag structure obviously increased the normalized reflectivity magnitude by 50% for all samples after 24 hours compared to the SPR structure with the addition of AgSiN/SU-8 layer. The minimum reflection of Cr/Ag/AgSiN/SU-8 structure changed only by approximately 5.26% for all samples, hence specifying the potential of the AgSiN/SU-8 layer to extend the SPR sensing characteristic. The increase in minimum reflectivity magnitude occurred due to the presence of oxygen element on the SPR sensing surface, which can be identified by FESEM analysis.

B. SPR SENSING CHARACTERISTIC

In this work, the characteristic of the SPR signal was conducted by calculating the sensitivity and the FWHM for Cr/Ag and Cr/Ag/AgSiN/SU-8 structures. FWHM was measured from the width of the SPR curve at half of its maximum amplitude to investigate the potential of the SPR structure's selectivity [37]. A sharper and narrow SPR curve will create a smaller FWHM value, which represents an excellent selectivity owing to the improvement in the resolution of the SPR structure [38]. For angular modulation scheme, the sensitivity of the SPR signal is described by the ratio of the changes in resonance angle to the changes in refractive index in the sensing medium [39]:

$$Sensitivity\left(\frac{^{\circ}}{RIU}\right) = \frac{\Delta\theta_{sp}}{\Delta n_s} \tag{5}$$

The sensitivity of the SPR structure is achieved by deriving the linear fitting expression for each sample variation, as shown in Figure 11. It is expressed that the Cr/Ag structure produces a smaller FWHM value and higher angular sensitivity than that of the Cr/Ag/AgSiN/SU-8 structure, as outlined in Table 2. The increase in the total thickness of the sensing layer causes a broader and shallow SPR curve, thus leading to an increment in the FWHM value and reducing the sensitivity of the SPR structure. However, the Cr/Ag/AgSiN/SU-8 structure has proven its potential in protecting the silver metal from eroding and provides a similar resonance angle with the smallest changes in reflectivity magnitude after 24 hours of application. For future work, the thickness of the sensing layer can be optimized to improve the SPR characteristic of the Cr/Ag/AgSiN/SU-8 structure.

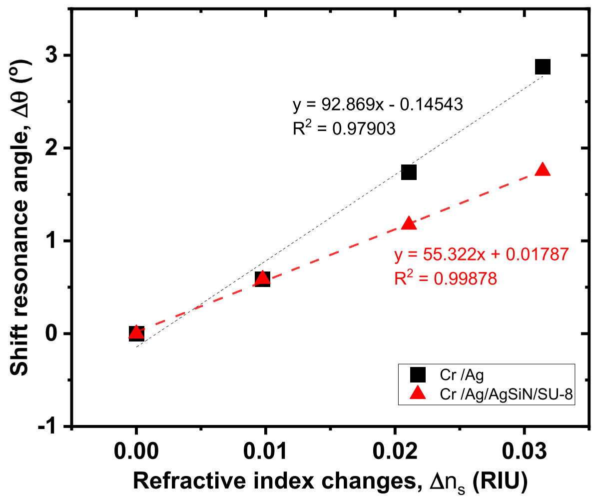

FIGURE 11. The shift of resonance angle as a function of refractive index changes in honey sample.

TABLE 2. Sensitivity and FWHM of the SPR structures.

SPR structure	Sensitivity (°/RIU)	Water content in honey (%)	FWHM (°)
Cr/Ag	92.869	30	0.81509
		26	0.74099
		22	0.66689
		18	0.59279
Cr/Ag/AgSiN/SU-8	55.322	30	1.36343
		26	1.33607
		22	1.30415
		18	1.24487

C. FESEM ANALYSIS

Table 3 describes the EDS analysis from the Field Emission Scanning Electron Microscopy (FESEM) system to determine the existence of atomic element in the SPR structure. The changes in minimum reflectivity after 24 hours in the Cr/Ag layer occurred due to the presence of 30.52% oxygen atomic percentage which might lead to the formation of silver oxide on the silver surface. The oxidized Cr/Ag layer yields small sporadic holes on the film and the possibility of substantial surface roughness, as shown in Figure 12 (a). In the meantime, the 21.48% reduction in the atomic oxygen of Cr/Ag/AgSiN/SU-8 structure proves that the additional layer of AgSiN/SU-8 film provides a great oxidation resistance to the silver surface. Thus, the formation of the silver oxide becomes more difficult, and the oxidation of the silver layer can be reduced. Furthermore, a merge surface that is crack-free and decreases in surface roughness was observed from Cr/Ag/AgSiN/SU-8 sensing surface, as depicted in Figure 12 (b).

TABLE 3. **Atomic percentage from EDS analysis after 24 hours.**

SPR structure	Element	Atomic percentage (%)
Cr/Ag	O	30.52
	Cr	9.35
	Ag	60.12
Cr/Ag/AgSiN/SU-8	N	43.61
	O	9.04
	Si	27.49
	Cr	1.54
	Ag	18.32

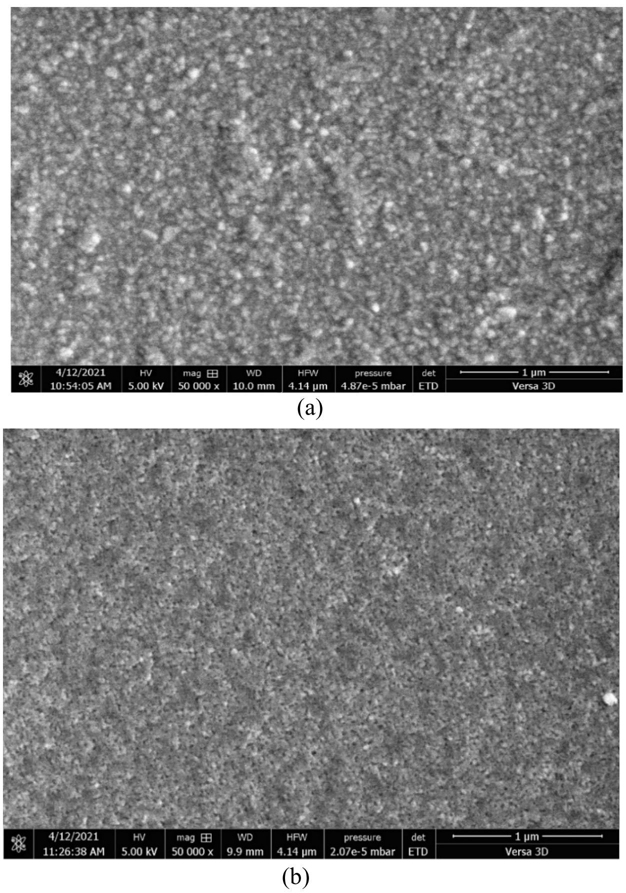

FIGURE 12. **Surface morphology of the (a) Cr/Ag and (b) Cr/Ag/AgSiN/SU-8 sensing layer.**

D. UV-VIS ANALYSIS

Figure 13 presents a UV-Vis analysis of both SPR structures with and without AgSiN/SU-8 layer. The absorbance spectrum retrieved from UV-Vis spectroscopy was used to measure the optical band gap using Tauc plot method. The band gap was measured to identify the minimum amount of energy required to excite an electron from valence band to the conduction band. Based on the finding, the optical band gap of Cr/Ag/AgSiN/SU-8 is lower than Cr/Ag by 2.985% which is deduced to affect the magnitude of the total reflectance. Therefore, the possibility of increasing the magnitude of the sensing sample's absorption can be achieved owing to the smaller band gap size and enough photon energy.

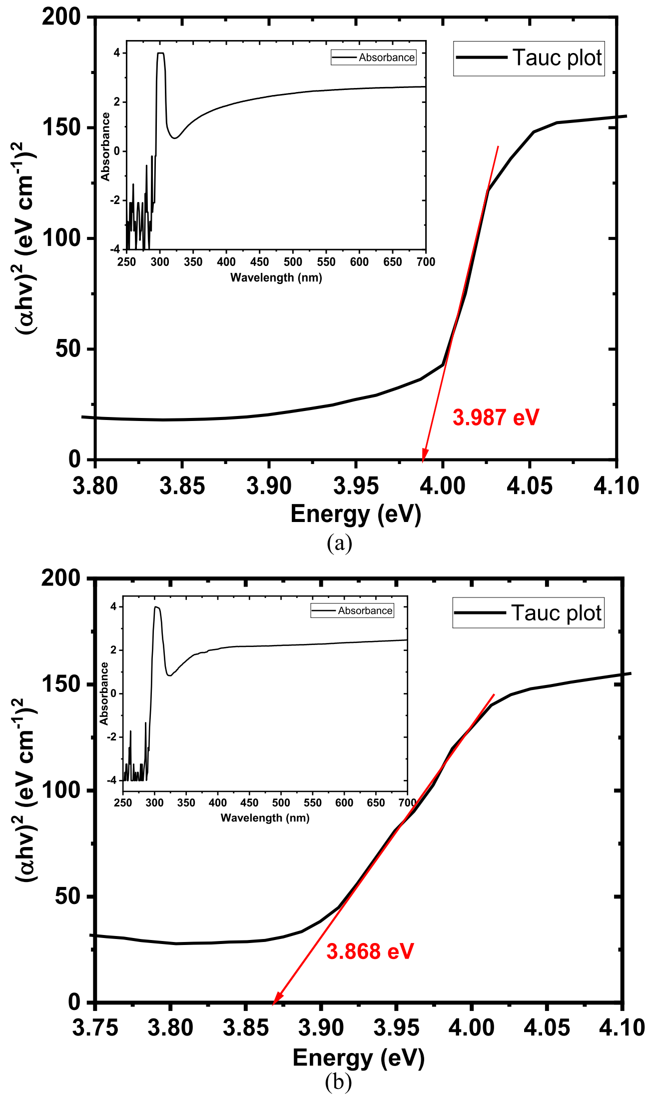

FIGURE 13. **UV-Vis analysis of the (a) Cr/Ag and (b) Cr/Ag/AgSiN/SU-8 structure from the absorbance spectrum using Tauc plot technique.**

V. CONCLUSION

The effect of AgSiN/SU-8 layer on silver-based prism-coupled SPR was examined for honey water content detection. The conclusion of results can be point as follow:

- All the resonance angles of adulterated honey solutions denote a similar behavior by shifting to a higher angle from the pure honey solution.
- The shift in resonance angle reveals the capability of the SPR structures to select and detect the variation percentage of honey water content.
- The higher concentration of honey solution carries a lower percentage of water content with a greater refractive index value, hence shifting the resonance angle to a higher degree.

- The AgSiN/SU-8 layer verifies its potential to protect the silver layer from erosion and preserve the SPR characteristic through a similar resonance angle value with only 5.26% changes in minimum reflection after 24 hours.
- The ability of the AgSiN/SU-8 layer to have good oxidation resistance was demonstrated by the 21.48% decrease in oxygen atomic percentage.
- The possibility of sensing sample's absorption magnitude was increased by lowering the 2.985% of band gap size from the Cr/Ag structure.

However, future work is required to build a sharper dip SPR curve and minimum reflectivity so as can enhance the SPR characteristic in terms of sensitivity and FWHM.

ACKNOWLEDGMENT

This research was supported by Universiti Tun Hussein Onn Malaysia (UTHM) through Tier 1 (vot Q485).

REFERENCES

[1] M. Yaacob, N. F. Rajab, S. Shahar, and R. Sharif, "Stingless bee honey and its potential value: A systematic review," *Food Res.*, vol. 2, no. 2, pp. 124–133, Nov. 2017, doi: 10.26656/fr.2017.2(2).212.

[2] P. V. Rao, K. T. Krishnan, N. Salleh, and S. H. Gan, "Biological and therapeutic effects of honey produced by honey bees and stingless bees: A comparative review," *Revista Brasileira de Farmacognosia*, vol. 26, no. 5, pp. 657–664, Sep. 2016, doi: 10.1016/j.bjp.2016.01.012.

[3] P. L. Miorin, N. C. L. Junior, A. R. Custodio, W. A. Bretz, and M. C. Marcucci, "Antibacterial activity of honey and propolis from *Apis mellifera* and *Tetragonisca angustula* against *Staphylococcus aureus*," *J. Appl. Microbiol.*, vol. 95, no. 5, pp. 913–920, Nov. 2003, doi: 10.1046/j.1365-2672.2003.02050.x.

[4] J. A. Nweze, J. I. Okafor, E. I. Nweze, and J. E. Nweze, "Evaluation of physicochemical and antioxidant properties of two stingless bee honeys: A comparison with *Apis mellifera* honey from Nsukka, Nigeria," *BMC Res. Notes*, vol. 10, no. 1, pp. 1–6, Dec. 2017, doi: 10.1186/s13104-017-2884-2.

[5] M. A. A. Jalil, A. R. Kasmuri, and H. Hadi, "Stingless bee honey, the natural wound healer: A review," *Skin Pharmacol. Physiol.*, vol. 30, no. 2, pp. 66–75, 2017, doi: 10.1159/000458416.

[6] F. Ij, M. H. Ab, I. Salwani, and M. Lavaniya, "Physicochemical characteristics of Malaysian stingless bee honey from Trigona species," *IIUM Med. J. Malaysia*, vol. 17, no. 1, pp. 187–191, Jul. 2018.

[7] A. F. Omar, O. K. M. Yahaya, K. C. Tan, M. H. Mail, and A. Seeni, "The influence of additional water content towards the spectroscopy and physicochemical properties of genus *Apis* and stingless bee honey," *Proc. SPIE*, vol. 9899, pp. 1–6, Apr. 2016, doi: 10.1117/12.2227060.

[8] *Revised Codex Standard for Honey, Standards and Standard Methods*, Codex Alimentarius Commission, Rome, Italy, 2001, doi: 10.1007/978-3-540-88242-8.

[9] T. Woodcock, G. Downey, J. D. Kelly, and C. O'Donnell, "Geographical classification of honey samples by near-infrared spectroscopy: A feasibility study," *J. Agricult. Food Chem.*, vol. 55, no. 22, pp. 9128–9134, Oct. 2007.

[10] D. Bertelli, M. Lolli, G. Papotti, L. Bortolotti, G. Serra, and M. Plessi, "Detection of honey adulteration by sugar syrups using one-dimensional and two-dimensional high-resolution nuclear magnetic resonance," *J. Agric. Food Chem.*, vol. 58, no. 15, pp. 8495–8501, 2010.

[11] R. D. O. R. Ribeiro, E. T. Mársico, C. D. S. Carneiro, M. L. G. Monteiro, C. C. Júnior, and E. F. O. D. Jesus, "Detection of honey adulteration of high fructose corn syrup by low field nuclear magnetic resonance (LF 1H NMR)," *J. Food Eng.*, vol. 135, pp. 39–43, Aug. 2014.

[12] H. Rybak-Chmielewska, "High performance liquid chromatography (HPLC) study of sugar composition in some kinds of natural honey and winter stores processed by bees from starch syrup," *J. Apicultural Sci.*, vol. 51, no. 1, pp. 23–38, 2007.

[13] M. M. Wheeler and G. E. Robinson, "Diet-dependent gene expression in honey bees: Honey vs. sucrose or high fructose corn syrup," *Sci. Rep.*, vol. 4, no. 1, Jul. 2014, Art. no. 5726, doi: 10.1038/srep05726.

[14] C. Cordella, J. S. L. T. Militão, M.-C. Clément, P. Drajnudel, and D. Cabrol-Bass, "Detection and quantification of honey adulteration via direct incorporation of sugar syrups or bee-feeding: Preliminary study using high-performance anion exchange chromatography with pulsed amperometric detection (HPAEC-PAD) and chemometrics," *Anal. Chim. Acta*, vol. 531, no. 2, pp. 239–248, Feb. 2005, doi: 10.1016/j.aca.2004.10.018.

[15] G. J. Padovan, D. De Jong, L. P. Rodrigues, and J. S. Marchini, "Detection of adulteration of commercial honey samples by the $^{13}C/^{12}C$ isotopic ratio," *Food Chem.*, vol. 82, no. 4, pp. 633–636, 2003, doi: 10.1016/S0308-8146(02)00504-6.

[16] X. Zhou, M. P. Taylor, H. Salouros, and S. Prasad, "Authenticity and geographic origin of global honeys determined using carbon isotope ratios and trace elements," *Sci. Rep.*, vol. 8, no. 1, Oct. 2018, Art. no. 14639, doi: 10.1038/s41598-018-32764-w.

[17] N. Irawati, N. M. Isa, A. F. Mohamed, H. A. Rahman, S. W. Harun, and H. Ahmad, "Optical microfiber sensing of adulterated honey," *IEEE Sensors J.*, vol. 17, no. 17, pp. 5510–5514, Sep. 2017, doi: 10.1109/JSEN.2017.2725910.

[18] N. Hida, N. Bidin, M. Abdullah, and M. Yasin, "Fiber optic displacement sensor for honey purity detection in distilled water," *Optoelectron. Adv. Mater. Commun.*, vol. 7, nos. 7–8, pp. 565–568, 2013, doi: 10.11113/jt.v74.4711.

[19] N. Hida, M. Abdullah, and M. Yasin, "Fiber optic displacement sensor for honey purity detection using glucose adulterant," *Jurnal Teknologi*, vol. 74, no. 8, pp. 1–4, Jun. 2015.

[20] R. M. Kingsta, M. Shamilee, and S. Sarumathi, "Detection of adulteration in honey using optical sensor," *Int. J. Adv. Res. Electr. Electron. Instrum. Eng.*, vol. 7, no. 3, pp. 1234–1241, 2018, doi: 10.15662/IJAREEIE.2018.0703032.

[21] N. H. Zainuddin, Y. W. Fen, A. A. Alwahib, M. H. Yaacob, N. Bidin, N. A. S. Omar, and M. A. Mahdi, "Detection of adulterated honey by surface plasmon resonance optical sensor," *Optik*, vol. 168, pp. 134–139, Sep. 2018, doi: 10.1016/j.ijleo.2018.04.048.

[22] W. M. Mukhtar, N. R. Ayob, R. M. Halim, N. D. Samsuri, N. F. Murat, A. R. A. Rashid, and K. A. Dasuki, "Effect of noble metal thin film thicknesses on surface plasmon resonance (SPR) signal amplification," *J. Adv. Res. Mater. Sci.*, vol. 49, no. 1, pp. 1–9, 2018.

[23] B. H. Ong, X. Yuan, S. C. Tjin, J. Zhang, and H. M. Ng, "Optimised film thickness for maximum evanescent field enhancement of a bimetallic film surface plasmon resonance biosensor," *Sens. Actuators B, Chem.*, vol. 114, no. 2, pp. 1028–1034, Apr. 2006, doi: 10.1016/j.snb.2005.07.064.

[24] S. H. Choi and K. M. Byun, "Investigation on an application of silver substrates for sensitive surface plasmon resonance imaging detection," *J. Opt. Soc. Amer. A, Opt. Image Sci.*, vol. 27, no. 10, pp. 2229–2236, 2010, doi: 10.1364/josaa.27.002229.

[25] S. Zynio, A. Samoylov, E. Surovtseva, V. Mirsky, and Y. Shirshov, "Bimetallic layers increase sensitivity of affinity sensors based on surface plasmon resonance," *Sensors*, vol. 2, no. 2, pp. 62–70, Feb. 2002, doi: 10.3390/s20200062.

[26] A. Verma, A. Prakash, and R. Tripathi, "Sensitivity enhancement of surface plasmon resonance biosensor using graphene and air gap," *Opt. Commun.*, vol. 357, pp. 106–112, Dec. 2015, doi: 10.1016/j.optcom.2015.08.076.

[27] I. J. C. D. L. Queiroz, A. A. D. Melo, F. P. M. Fernandes, F. D. C. Fim, S. Blair, Y. Wang, C. D. S. Moreira, and R. M. S. Cruz, "Sensitivity enhancement of silver-based SPR sensors using ultrathin gold film and graphene overlay," in *Proc. IEEE Int. Instrum. Meas. Technol. Conf. (I2MTC)*, May 2020, pp. 1–6, doi: 10.1109/I2MTC43012.2020.9129151.

[28] N. H. Kim, M. Choi, T. W. Kim, W. Choi, S. Y. Park, and K. M. Byun, "Sensitivity and stability enhancement of surface plasmon resonance biosensors based on a large-area Ag/MoS_2 substrate," *Sensors*, vol. 19, no. 1894, pp. 1–8, 2019, doi: 10.3390/s19081894.

[29] N. A. Jamil, G. S. Mei, N. B. Khairulazdan, S. P. Thiagarajah, A. A. Hamzah, B. Y. Majlis, and P. S. Menon, "Detection of uric acid using Kretschmann-based SPR biosensor with MoS_2-graphene," in *Proc. IEEE Student Conf. Res. Develop. (SCOReD)*, Nov. 2018, pp. 1–4, doi: 10.1109/SCORED.2018.8710842.

[30] G. Mohanty and B. K. Sahoo, "III–V nitrides and graphene SPR biosensor for hemoglobin detection," in *Progress in Optomechatronics*, vol. 249. Singapore: Springer, 2020, doi: 10.1007/978-981-15-6467-3_5.

[31] G. Mohanty and B. K. Sahoo, ''III–V nitrides and performance of graphene on copper plasmonic biosensor,'' *Superlattices Microstruct.*, vol. 93, pp. 226–233, May 2016, doi: 10.1016/j.spmi.2016.03.040.

[32] G. Mohanty, J. Akhtar, and B. K. Sahoo, ''Effect of semiconductor on sensitivity of a graphene-based surface plasmon resonance biosensor,'' *Plasmonics*, vol. 11, no. 1, pp. 189–196, Feb. 2016, doi: 10.1007/s11468-015-0033-0.

[33] Z. Yang, J. Wang, Y. Shao, Y. Jin, and M. Yi, ''Studying corrosion of silver thin film by surface plasmon resonance technique,'' *Opt. Quantum Electron.*, vol. 52, no. 1, pp. 1–8, Jan. 2020, doi: 10.1007/s11082-019-2156-6.

[34] O. Pluchery, R. Vayron, and K.-M. Van, ''Laboratory experiments for exploring the surface plasmon resonance,'' *Eur. J. Phys.*, vol. 32, no. 2, pp. 585–599, Mar. 2011, doi: 10.1088/0143-0807/32/2/028.

[35] Y. W. Fen and W. M. M. Yunus, ''Characterization of the optical properties of heavy metal ions using surface plasmon resonance technique,'' *Opt. Photon. J.*, vol. 1, no. 3, pp. 116–123, 2011, doi: 10.4236/opj.2011.13020.

[36] S. Franssila, *Introduction to Microfabrication*, 2nd ed. Hoboken, NJ, USA: Wiley, 2010.

[37] W. M. Mukhtar, R. M. Halim, and H. Hassan, ''Optimization of SPR signals: Monitoring the physical structures and refractive indices of prisms,'' in *Proc. EPJ Web Conf.*, vol. 162, 2017, pp. 1–5, doi: 10.1051/epjconf/201716201001.

[38] A. Paliwal, A. Sharma, M. Tomar, and V. Gupta, ''Surface plasmon resonance study on the optical sensing properties of tin oxide (SnO_2) films to NH_3 gas,'' *J. Appl. Phys.*, vol. 119, no. 16, pp. 1–10, Apr. 2016, doi: 10.1063/1.4948332.

[39] Z. Lin, L. Jiang, L. Wu, J. Guo, X. Dai, Y. Xiang, and D. Fan, ''Tuning and sensitivity enhancement of surface plasmon resonance biosensor with graphene covered Au-MoS_2-Au films,'' *IEEE Photon. J.*, vol. 8, no. 6, pp. 1–8, Dec. 2016, doi: 10.1109/JPHOT.2016.2631407.

M. B. JAAFAR was born in Kuala Lumpur, Malaysia, in April 1991. She received the degree from the Kedah Technical Matriculation College, Pendang, Kedah, Malaysia, the B.Eng. degree (Hons.) in electronic engineering, in 2014, and the master's degree (by research) in electronic engineering and the Ph.D. degree in optical sensing engineering from the University of Tun Hussein Onn Malaysia, Batu Pahat, Johor, in 2017 and 2023, respectively.

Her research interest includes the scope of photonic communication engineering.

M. B. OTHMAN (Member, IEEE) received the B.Eng. degree (Hons.) in computer system and communication engineering and the M.Sc. degree in communication network engineering from Universiti Putra Malaysia (UPM), in 2001 and 2005, respectively, and the Ph.D. degree in metro-access and short-range system from DTU Fotonik, Technical University of Denmark, in 2012.

She is currently an Associate Professor and a Fellow Researcher with the Advanced Telecommunication Research Center (ATRC), Faculty of Electrical and Electronic Engineering (FKEE), Universiti Tun Hussein Onn Malaysia. Her research interests include advanced modulation formats, photonic wireless integration and access, in-home network technologies, and immersive technologies.

M. M. I. MEGAT HASNAN received the Bachelor of Telecommunication Engineering and the Master of Engineering Science degrees in microelectromechanical (MEMs) design and the Ph.D. degree in engineering science in renewable energy from the University of Malaya, Malaysia, in 2011, 2015, and 2019, respectively.

He is currently a Senior Lecturer with the Faculty of Engineering, University Malaysia Sabah (UMS).

H. HAROON (Member, IEEE) received the B.Eng. and M.Eng. degrees in electrical engineering from Universiti Teknologi Malaysia (UTM), Malaysia, in 2001 and 2004, respectively, and the Ph.D. degree from Universiti Kebangsaan Malaysia (UKM), Malaysia.

She has been in the teaching profession, since 2002. She is currently a Senior Lecturer with the Faculty of Electronics and Computer Engineering, Universiti Teknikal Malaysia Melaka (UTeM). Her research interests include microengineering, photonics, and optical communications.